Journal of Alloys and Compounds 489 (2010) 146–151

Contents lists available at ScienceDirect

Journal of Alloys and Compounds

journal homepage: www.elsevier.com/locate/jallcom

Thermodynamic assessments of Ag–Dy and Ag–Er binary systems

Z.H. Long[a], Y.J. Yang[a], S. Jin[a], H.S. Liu[a,b,*], F. Zheng[a,b], Z.P. Jin[a,b]

[a] School of Materials Science and Engineering, Central South University, Changsha, Hunan Province, 410083, PR China
[b] The Key Lab of Non-Ferrous Metal Materials Science and Engineering, Ministry of Education, PR China

ARTICLE INFO

Article history:
Received 20 May 2009
Received in revised form 8 September 2009
Accepted 9 September 2009
Available online 16 September 2009

Keywords:
Thermodynamic calculation
Ag–Dy system
Ag–Er system
CALPHAD

ABSTRACT

Thermodynamic assessments of Ag–Dy and Ag–Er binary systems have been performed by using CALPHAD method. In order to provide necessary data for thermodynamic assessment, the formation enthalpies of Ag_2Dy, AgDy, Ag_2Er and AgEr were calculated by using projector augmented-wave (PAW) method within generalized gradient approximation (GGA) in first-principles frame. During assessments of the Ag–Dy and Ag–Er binary systems, the solution phases (liquid, fcc and hcp) were treated as substitutional solutions, of which the excess Gibbs energies were modeled by Redlich–Kister polynomial, and all intermetallic compounds were described as stoichiometric phases. Consequently, phase diagrams of these two binary systems were thermodynamically optimized and the self-consistent thermodynamic parameters of involved phases obtained.

1. Introduction

Ag-based alloys with high electronic-conductivity have found wide application in electronic industry. However, many Ag-based alloys are of poor strength and cannot withstand high temperature. Fortunately, addition of some rare-earth elements into Ag-based alloys may help to achieve high strength and improve their performances at elevated temperature [1]. Besides, silver and rare-earth are important components of several amorphous materials [2]. Information of phase diagrams of the Ag–RE systems is helpful to alloys design relevant processing method. Recently, many assessments about Ag–RE systems have been carried out, including Ag–La [3], Ag–Pr [4], Ag–Ce [5], Ag–Gd [6,7], Ag–Nd [7,8], Ag–Yb [9], Ag–Eu [10], Ag–Y [11], Ag–Sc [12], Ag–Sm [13], Ag–Tb and Ag–Ho [14]. However, the Ag–Dy and Ag–Er systems have not been optimized despite their importance. In order to construct a integrated thermodynamic database of Ag–RE systems which are of help to related materials design, thermodynamic assessments of Ag–Dy and Ag–Er phase diagrams are performed through CALPHAD approach with the help of first-principles calculations in this work.

2. Evaluation of experiment data

2.1. Ag–Dy system

With the help of metallography, X-ray diffraction (XRD) and differential thermal analysis (DTA), Delfino et al. [15] previously constructed the phase diagram of Ag–Dy system. Three compounds, i.e. $Ag_{51}Dy_{14}$, Ag_2Dy and AgDy, were reported. Meanwhile four eutectic reactions were detected. Gschneidner et al. [16] measured the maximum solid solubility of Dy in Ag to be 1.3 at.%, and determined the eutectic temperature of $L \leftrightarrow Fcc(Ag) + Ag_{51}Dy_{14}$ as 1074 K.

As for thermodynamic properties, only the formation enthalpies of the compounds were reported. By using high temperature direct synthesis calorimetry, Meschel and Kleppa [17] measured the formation enthalpies of $Ag_{51}Dy_{14}$, Ag_2Dy and AgDy at 1373 ± 2 K. However, the formation enthalpy of Ag_2Dy in Ref. [17] was a little higher. This means it might decompose at low temperature, implying confliction with the experimental phase diagrams [15]. Due to lack of other argument, we think that the phase stability [15] is more reliable than the measured formation enthalpy. Other thermodynamic property of Ag–Dy system has not been reported so far. In order to get a reliable description, first-principles calculations should be utilized. In this work, Ag_2Dy and AgDy will be selected to determine the formation enthalpies. As for $Ag_{51}Dy_{14}$, because too many atoms are involved in a unit cell, and the imperfect site occupancy, it is very difficult to calculate the formation enthalpy of $Ag_{51}Dy_{14}$ using first-principles.

* Corresponding author at: School of Materials Science and Engineering, Central South University, Changsha, Hunan Province, 410083, PR China. Tel.: +86 731 88876 735; fax: +86 731 88876 692.
E-mail address: hsliu@mail.csu.edu.cn (H.S. Liu).

0925-8388/$ – see front matter © 2009 Elsevier B.V. All rights reserved.
doi:10.1016/j.jallcom.2009.09.036

2.2. Ag–Er system

The melting point of Ag and Er in this work are accepted as 1235 and 1802 K [18,19], respectively. Through DTA, metallography and various X-ray methods, Gebhardt et al. [20] studied the Ag–Er phase diagram. Three congruently melting compounds and four eutectic reactions were reported. Note the melting point reported by Gebhardt et al. [20] for Er was 29 K lower than the accepted value due to the lower purity of Er (99% Er) used in the experiments [20]. Mcmasters et al. [21] studied the crystal structure of the Ag-rich compound in this system and determined it to be $Ag_{51}Er_{14}$ with the hexagonal structure. Gschneidner et al. [16] investigated the solid solubility of Er in Ag and the Ag-rich eutectic temperature. The solubility of Er in Ag was 3.6 at.% [16], slightly higher than the value reported by Bijvoet et al. [22].

Meschel and Kleppa [17] measured the formation enthalpies of $Ag_{51}Er_{14}$, Ag_2Er and AgEr in Ag–Er binary system at 1373 ± 2 K. Like in the Ag–Dy system, the enthalpy of Ag_2Er in Ref. [17] looks a little higher, indicating its metastability at low temperature. This conflicts with the widely accepted phase relations at solid state [20]. In this work, more attentions have been paid to the experimental phase diagram [20] than the measured enthalpy. With the same reason mentioned for the Ag–Dy system (see Section 2.1), only the formation enthalpies of Ag_2Er and AgEr will be calculated by first-principles calculations.

3. First-principles calculations

The first-principles calculations were executed using the scalar relativistic all-electron Blöchl's projector augmented-wave (PAW) [23,24] method within the generalized gradient approximation (GGA), as implemented in the highly efficient Vienna ab initio simulation package (VASP) [25,26]. The Perdew–Wang parameterization (PW91) [27,28] was employed in the GGA exchange-correlation function. For the four intermetallic compounds, Ag_2Dy, AgDy, Ag_2Er and AgEr, the plane-wave energy cutoff was 400 eV. Brillouin zone integrations were performed using Monkhorst–Pack. k-Point meshes and reciprocal space (k-point) meshes are increased to achieve convergence to a precision of 0.3 kJ/mol of atom. The k-point meshes for these four compounds were fixed to $11 \times 11 \times 11$. The total energy was converged numerically to less than 1×10^{-6} eV/unit with respect to electronic, ionic and unit cell degrees of freedom. The latter two relaxed using Hellman–Feymann forces with a preconditioned conjugated gradient algorithm. After structural optimization, the total forces on each ion were less than 0.01 eV/Å. In order to avoid wrap-around errors, all calculations are performed using the "high" setting within VASP.

The formation enthalpies for the intermetallic compounds were calculated by the following equation

$$\Delta H(\mathrm{Ag}_x\mathrm{M}_y) = E_{\mathrm{total}}(\mathrm{Ag}_x\mathrm{M}_y) - xE_{\mathrm{total}}(\mathrm{Ag}) - yE_{\mathrm{total}}(\mathrm{M}) \quad (1)$$

here $E_{\mathrm{total}}(\mathrm{Ag}_x\mathrm{M}_y)$, $E_{\mathrm{total}}(\mathrm{Ag})$ and $E_{\mathrm{total}}(\mathrm{M})$ are the calculated total energies (per atom at $T = 0$ K) of the intermetallic compound, pure Ag, pure Dy or Er, respectively. In this work, the formation enthalpies of the compounds calculated by first-principles were assumed to be the values of the corresponding phases at 298 K.

4. Thermodynamic model

An ordinary substitution solution model is employed to describe liquid, fcc and hcp solution. The molar Gibbs energy of a solution phase (Φ = liquid, fcc, hcp) can be represented as a sum of the weighted Gibbs energy for the pure elements, the ideal entropy term describing a random mixing of the components, and the excess Gibbs energy describing the degree of deviation from ideal mixing, i.e.

$$G_{\mathrm{m}}^{\Phi} = \sum x_{\mathrm{i}}{}^{0}G_{\mathrm{i}}^{\Phi} + RT\sum x_{\mathrm{i}}\ \ln(x_{\mathrm{i}}) + {}^{E}G_{\mathrm{m}}^{\Phi} \quad (2)$$

where G_{m}^{Φ} is the molar Gibbs energy of a solution phase Φ, ${}^{0}G_{\mathrm{i}}^{\Phi}$ the Gibbs energy of pure element i (i = Ag, Dy or Ag, Er) in the structural state of Φ, R the gas constant, and T temperature. And the excess Gibbs energy, ${}^{E}G_{\mathrm{m}}^{\Phi}$, can be expressed by the Redlich–Kister polynomial functions as follows:

$${}^{E}G_{\mathrm{m}}^{\Phi} = x_{\mathrm{Ag}}x_{\mathrm{M}}\sum_{j=0}^{n}{}^{(j)}L_{\mathrm{Ag,M}}^{\Phi}(x_{\mathrm{Ag}} - x_{\mathrm{M}})^{j} \quad (3)$$

Here M stands for either Dy or Er, ${}^{(j)}L_{\mathrm{Ag,M}}^{\Phi}$ an interaction parameter and can be expressed as follows:

$${}^{(j)}L_{\mathrm{Ag,M}}^{\Phi} = A_j + B_jT \quad (4)$$

here A_j and B_j are model parameters to be optimized.

The intermetallic compounds were treated as stoichiometric phases $\mathrm{Ag_pM_q}$. Due to lack of heat capacity data and according to the Neumann–Kopp rule, the Gibbs energy of $\mathrm{Ag_pM_q}$ can be formulated as:

$$G_{\mathrm{Ag_pM_q}} = \frac{p}{p+q}{}^{0}G_{\mathrm{Ag}}^{\mathrm{fcc}} + \frac{q}{p+q}{}^{0}G_{\mathrm{M}}^{\mathrm{hcp}} + A + BT \quad (5)$$

where A and B are the parameters to be optimized in this work.

5. Results and discussion

5.1. First-principle calculations

Crystal structures, lattice constants and formation enthalpies of intermetallic compounds are listed in Table 1. The lattice constants of pure elements were previously calculated with first-principles method by Wang et al. [29]. It is clear that the results obtained in present calculation are in good agreement with those calculated by Wang et al. [29]. Moreover, the obtained lattice constants of pure elements agree reasonably well with those experiment data [18,30,31]. The thermodynamic properties of these intermetallic compounds were further calculated in this work. As seen in Table 1, the calculated lattice constants of four intermetallic compounds are in good agreement with experimental data from literatures [32,33]. In view of these, it is reasonable to accept the formation enthalpies of these compounds obtained by first-principles calculations.

5.2. Phase diagram

Besides the lattice stabilities of Dy and Er of face centered cubic (fcc) structure were cited from Wang et al. [35] and Du et al. [36], respectively, those in other structures were taken from Dinsdale [37]. Using PARROT module of Thermo-Calc program, thermodynamic parameters of all phases in these two systems are obtained and listed in Table 2. As can be seen in the next paragraphs, most experimental data including phase diagrams and thermodynamic properties can be reproduced.

5.2.1. Ag–Dy system

Fig. 1 illustrates the calculated phase diagram of Ag–Dy system compared with experimental data, and Table 3 lists the invariant reactions in Ag–Dy system. The calculated boundaries agree with the experimental data considering the measurement errors. The largest temperature deviation between the calculated and experimental values for invariant reactions is within 9 K.

Fig. 2 shows the calculated formation enthalpies of intermetallic compounds at 298 K versus data of experimental [17], prediction [38] and those obtained by first-principles. We found those three

Table 1
Crystal structures and formation enthalpies of the compounds in Ag–Dy and Ag–Er systems by first-principles calculations.

Phase	Person symbol	Space group	Prototype	Lattice (Å)		ΔH (J/g atom)	Reference
				a	c		
Ag	$cF4$	$Fm\bar{3}m$	Cu	4.154	–	–	This work
				4.155	–	–	[29]
				4.086	–	–	[30]
Dy	$hP2$	$P6_3/mmc$	Mg	3.606	5.619	–	This work
				3.604	5.626	–	[29]
				3.588	5.646	–	[31]
Er	$hP2$	$P6_3/mmc$	Mg	3.575	5.541	–	This work
				3.576	5.543	–	[29]
				3.559	5.585	–	[18]
Ag_2Dy	$tI6$	$I4/mmm$	$MoSi_2$	3.754	9.259	−32,579	This work
				3.694	9.213	−22,300 ± 2,300	[32,17]
				–	–	−39,000	[38]
AgDy	$cP2$	$Pm\bar{3}m$	CsCl	3.639	–	−32,812	This work
				3.609	–	−37,300 ± 1,800	[33,17]
				–	–	−44,000	[38]
Ag_2Er	$tI6$	$I4/mmm$	$MoSi_2$	3.721	9.184	−34,119	This work
				3.669	9.155	−24,000 ± 2,300	[32,17]
				–	–	−39,000	[38]
AgEr	$cP2$	$Pm\bar{3}m$	CsCl	3.602	–	−34,488	This work
				3.584	–	−44,900 ± 3,200	[34,17]
				–	–	−44,000	[38]

compounds can be stable at room temperature according to the formation enthalpies calculated by both first-principles and CALPHA method and the results agree well with the experimental phase diagram [15]. Furthermore, the formation enthalpy of AgDy obtained by first-principles is also in agreement with the measured data [17] considering the experimental error. The assessed formation enthalpies of $Ag_{51}Dy_{14}$ and AgDy reasonably agree well with the data obtained by experiment [17] and first-principles, respectively, while the assessed formation enthalpy of Ag_2Dy agree well with the value from first-principles calculations.

5.2.2. Ag–Er system

Phase diagram of Ag–Er binary system was reproduced thermodynamically (Fig. 3) with all assessed invariant reactions listed in Table 4. Clearly, good agreement has been realized between experimental diagram and assessed boundaries. The largest temperature deviation between assessed and measured invariant reactions is within 8 K.

As shown in Fig. 4, the formation enthalpies of intermetallic compounds at 298 K were further assessed thermodynamically. Three compounds can be stable at room temperature according to the formation enthalpies calculated by first-principles and CALPHAD, which is in agreement with the experimental phase diagram [20]. The assessed formation enthalpies of $Ag_{51}Er_{14}$ and AgEr agree well with experimental data [17], while that of Ag_2Er is in agreement with the value from first-principles calculations. However, the calculated formation enthalpy of AgEr by first-principles differs from measured data [17]. Two possible reasons may contribute to this deviation. One of them is associated with the complicated electronic arrangement of rare-earth elements with less accurate

Table 2
Thermodynamic parameters of Ag–Dy and Ag–Er systems.

System	Phase	Thermodynamic parameters
Ag–Dy	Liquid	${}^0L^{Liq}_{Ag,Dy} = -120,882 + 21.174T$
		${}^1L^{Liq}_{Ag,Dy} = -69,962 + 27.008T$
		${}^2L^{Liq}_{Ag,Dy} = 27,773$
		${}^3L^{Liq}_{Ag,Dy} = 18,181$
	Fcc	${}^0L^{Fcc}_{Ag,Dy} = -65,136 - 5.743T$
	Hcp	${}^0L^{Hcp}_{Ag,Dy} = 100,000$
	$Ag_{51}Dy_{14}$	${}^0G^{Ag_{51}Dy_{14}} = 0.7846\,{}^0G^{Fcc}_{Ag} + 0.2154\,{}^0G^{Hcp}_{Dy} - 23,940 + 1.445T$
	Ag_2Dy	${}^0G^{Ag_2Dy} = 0.6667\,{}^0G^{Fcc}_{Ag} + 0.3333\,{}^0G^{Hcp}_{Dy} - 31,050 + 2.207T$
	AgDy	${}^0G^{AgDy} = 0.5\,{}^0G^{Fcc}_{Ag} + 0.5\,{}^0G^{Hcp}_{Dy} - 35,003 + 2.704T$
Ag–Er	Liquid	${}^0L^{Liq}_{Ag,Er} = -148,651 + 29.155T$
		${}^1L^{Liq}_{Ag,Er} = -59,235 + 10.186T$
		${}^2L^{Liq}_{Ag,Er} = 13,751$
		${}^3L^{Liq}_{Ag,Er} = 46,024$
	Fcc	${}^0L^{Fcc}_{Ag,Er} = -82,000$
	Hcp	${}^0L^{Hcp}_{Ag,Er} = 10,000$
	$Ag_{51}Er_{14}$	${}^0G^{Ag_{51}Er_{14}} = 0.7846\,{}^0G^{Fcc}_{Ag} + 0.2154\,{}^0G^{Hcp}_{Er} - 27,877 + 2.347T$
	Ag_2Er	${}^0G^{Ag_2Er} = 0.6667\,{}^0G^{Fcc}_{Ag} + 0.3333\,{}^0G^{Hcp}_{Er} - 35,335 + 2.077T$
	AgEr	${}^0G^{AgEr} = 0.5\,{}^0G^{Fcc}_{Ag} + 0.5\,{}^0G^{Hcp}_{Er} - 41,363 + 4.867T$

Table 3
Comparison of invariant reactions in the Ag–Dy system.

Reaction	Composition of liquid, X_{Dy}	T (K)	Type	Ref.
$L \leftrightarrow Fcc(Ag) + Ag_{51}Dy_{14}$	0.111	1075	Eutectic	This work
	0.120 ± 0.005	1073 ± 5	Eutectic	[15]
	–	1074	Eutectic	[16]
$L \leftrightarrow Ag_{51}Dy_{14} + Ag_2Dy$	0.275	1182	Eutectic	This work
	0.286 ± 0.005	1178 ± 5	Eutectic	[15]
$L \leftrightarrow Ag_2Dy + AgDy$	0.369	1223	Eutectic	This work
	0.375 ± 0.005	1223 ± 10	Eutectic	[15]
$L \leftrightarrow AgDy + Hcp(Dy)$	0.695	1171	Eutectic	This work
	0.745 ± 0.005	1173 ± 10	Eutectic	[15]
$L \leftrightarrow Ag_{51}Dy_{14}$	0.215	1254	Congruent	This work
	0.215	1263 ± 10	Congruent	[15]
$L \leftrightarrow Ag_2Dy$	0.333	1245	Congruent	This work
	0.333	1253 ± 10	Congruent	[15]
$L \leftrightarrow AgDy$	0.5	1464	Congruent	This work
	0.5	1458 ± 10	Congruent	[15]

Table 4
Comparison of invariant reactions in the Ag–Er system.

Reaction	Composition of liquid, X_{Er}	T (K)	Type	Ref.
$L \leftrightarrow Fcc(Ag) + Ag_{51}Er_{14}$	0.121	1060	Eutectic	This work
	0.115	1045	Eutectic	[20]
	–	1068	Eutectic	[16]
$L \leftrightarrow Ag_{51}Er_{14} + Ag_2Er$	0.258	1168	Eutectic	This work
	0.265	1163	Eutectic	[20]
$L \leftrightarrow Ag_2Er + AgEr$	0.374	1260	Eutectic	This work
	0.37	1266	Eutectic	[20]
$L \leftrightarrow AgEr + Hcp(Er)$	0.726	1199	Eutectic	This work
	0.76	1205	Eutectic	[20]
$L \leftrightarrow Ag_{51}Er_{14}$	0.215	1204	Congruent	This work
	0.215	1203	Congruent	[20]
$L \leftrightarrow Ag_2Er$	0.333	1295	Congruent	This work
	0.333	1293	Congruent	[20]
$L \leftrightarrow AgEr$	0.5	1476	Congruent	This work
	0.5	1468	Congruent	[20]

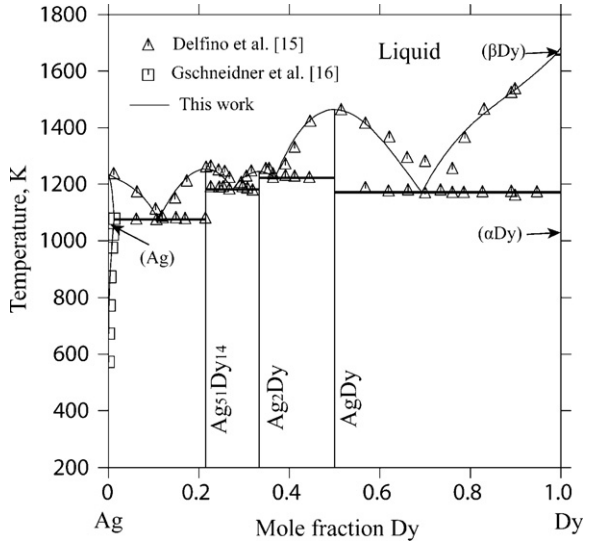

Fig. 1. The calculated Ag–Dy phase diagram with experimental data [15,16].

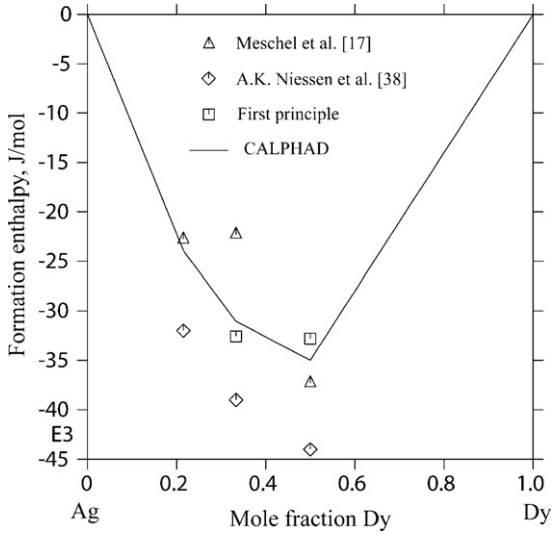

Fig. 2. Calculated formation enthalpies of the compounds compared with experimental data [17], predicted values [38] and values by first-principles calculations. Reference states: Fcc_A1 Ag and Hcp_A3 Dy.

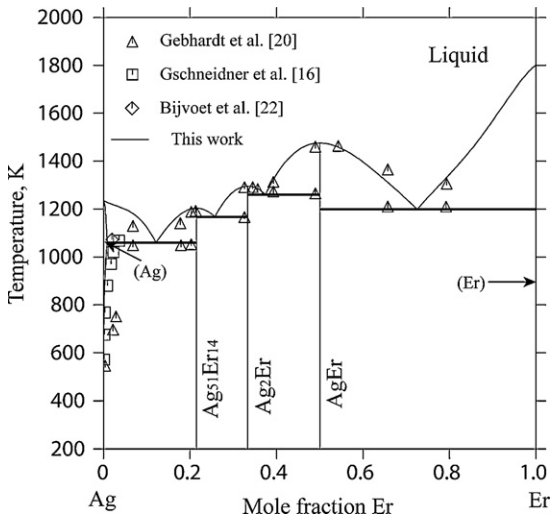

Fig. 3. The calculated Ag–Er phase diagram with experimental data [16,20,22].

potential functions. Another is owing to the activity of rare-earth elements. As we known, rare earth is easy to be oxidized. This may bring in inevitably error in the process of formation enthalpy measurement.

In addition, similar cases also appeared in Ag–Tb and Ag–Ho systems [14]. In these two systems, the measured formation enthalpies of Ag_2Tb and Ag_2Ho [17] also tend to be a bit higher. But they appear to be stable at low temperature in experimental phase diagrams [39,40]. In order to assure all the compounds to be stable, the assessed formation enthalpy of Ag_2Ho [14] was much lower than the measured data [17], while that of AgTb [14] to be higher than experimental value [17]. Especially, the measured formation enthalpy of AgTb [17] differed significantly from the experimental data in Ref. [41]. This indicates large error inevitably existing in the measured formation enthalpy of rare-earth compounds. So, it can be understood that difference exists between the calculated and experimental formation enthalpies.

To sum up, based on the following reasons, the formation enthalpies obtained by first-principles were adopted during assessment. First, the calculated formation enthalpies obtained by

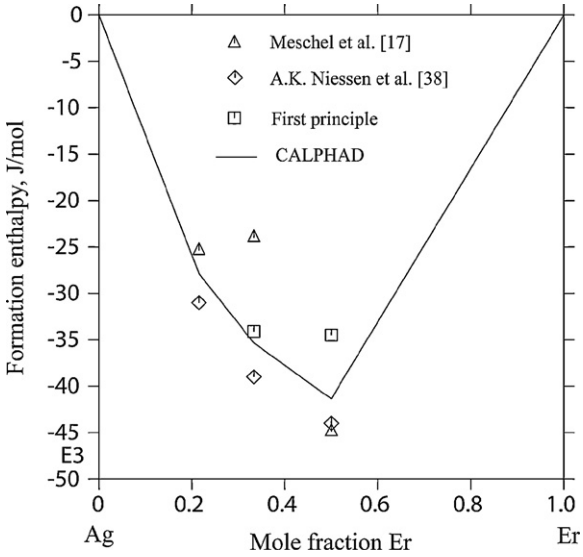

Fig. 4. Calculated formation enthalpies of the compounds compared with experimental data [17], predicted values [38] and values by first-principles calculations. Reference states: Fcc_A1 Ag and Hcp_A3 Er.

first-principles can fit with experimental phase diagrams [15,20], while the measured formation enthalpies [17] do not agree with them. Further experimental information of formation enthalpies or phase relations may be needed. But in this paper, the phase diagrams are regarded more reliably. Second, as can be seen from Fig. 2, if one lowers the experimental formation enthalpies of Ag_2Dy or increases the formation enthalpies of AgDy can avoid the above contrary. Our first-principles calculated results can just answer for such demand. This may suggest that the first-principles results are reasonable. Similar case happens in the Ag–Er system (Fig. 4). Besides, the calculated crystal structures and lattice constants of the pure elements and compounds in this work agree well with corresponding experimental data and the first-principles calculated results by Wang et al. [29]. In view of these, the formation enthalpies of these compounds obtained by first-principles calculations are reliable although there may be error in density function theory (DFT) when rare-earth elements being considered. At the same time, because the potentials of the elements with f-element are not accurate enough, the errors of the results by first-principles are inevitable. So, during assessment, both the measured and first-principles calculated formation enthalpies were adopted, but slightly larger weights were given to the results obtained by first-principles.

6. Conclusions

Phase diagrams of Ag–Dy and Ag–Er binary systems have been thermodynamically optimized based on experimental data and first-principles calculations of the phase equilibrium and thermodynamic properties. A set of self-consistent thermodynamic parameters for each system has been obtained, which can reproduces the phase diagram boundaries and thermodynamic data reasonably well.

Acknowledgments

This work was financially supported by National Science Foundation of China (No. 50671122) and Hunan Provincial Innovation Foundation for Postgraduate (No. 1343-74236000007). The optimization was carried out by using the Thermo-Calc program licensed from TCSAB, Sweden. The calculated results were checked using the Pandat program licensed from The CompuThermo, LLC, Madison, WI, USA.

References

[1] J.B. Liu, L. Zhang, L. Meng, Mater. Sci. Eng. A 498 (2008) 392–396.
[2] E.S. Park, H.G. Kang, W.T. Kim, D.H. Kim, J. Non-Crystall. Solids 279 (2001) 154–160.
[3] Z. Li, X.P. Su, F.C. Yin, C.T. Chen, J. Alloys Compd. 299 (2000) 195–198.
[4] F.C. Yin, X.P. Su, Z. Li, P. Zhang, M.H. Huang, Y. Shi, J. Alloys Compd. 307 (2000) 202–206.
[5] F.C. Yin, M.H. Huang, X.P. Su, P. Zhang, Z. Li, Y. Shi, J. Alloys Compd. 334 (2002) 154–158.
[6] H. Wang, L.G. Zhang, W.J. Zhu, H.S. Liu, Z.P. Jin, J. Alloys Compd. 466 (2008) 165–168.
[7] S.L. Wang, C.P. Wang, X.J. Liu, K. Ishida, J. Alloys Compd. 476 (2009) 245–252.
[8] G.X. Huang, L.G. Zhang, B.R. Jia, H.Y. Qi, L.B. Liu, Z.P. Jin, J. Alloys Compd 471 (2009) 176–179.
[9] L.G. Zhang, F.G. Meng, H.S. Liu, L.B. Liu, Z.P. Jin, J. Alloys Compd. 452 (2008) 304–306.
[10] L.G. Zhang, H.S. Liu, L.B. Liu, Z.P. Jin, J. Cent. South Univ. Technol. 14 (2007) 123–126.
[11] S.L. Wang, C.P. Wang, X.J. Liu, K. Ishida, J. Alloys Compd. 476 (2009) 187–192.
[12] X.J. Liu, S.L. Wang, C.P. Wang, J. Alloys Compd. 469 (2009) 186–192.
[13] S.L. Wang, C.P. Wang, X.J. Liu, The Program Booklet of the 14th National Conference and Multilateral Symposium on Phase Diagrams and Materials Design, Changsha, China, November 3–5, 2008, pp. 170–173.
[14] S.L. Wang, C.P. Wang, X.J. Liu, A.T. Tang, F.S. Pan, K. Ishida, J. Alloys Compd. (2009), doi:10.1016/j.jallcom.2009.04.037.
[15] S. Delfino, R. Ferro, R. Capelli, A. Borsese, J. Less-Common Met. 44 (1976) 267–271.

[16] K.A. Gschneidner Jr., O.D. Mcmasters, D.G. Alexander, R.F. Venterichter, Metall. Trans. 1 (1970) 1961–1971.
[17] S.V. Meschel, O.J. Kleppa, J. Alloys Compd. 376 (2004) 73–78.
[18] B.J. Beaudry, K.A. Gschneidner Jr., in: K.A. Gschneidner Jr., L. Eyring (Eds.), Handbook on the Physics and Chemistry of Rare Earths, vol. 1-Metals, North-Holland Publishing Co., Amsterdam, 1978, p. 215.
[19] D.C. Koskenmaki, K.A. Gschneidner Jr., in: K.A. Gschneidner Jr., L. Eyring (Eds.), Handbook on the Physics and Chemistry of Rare Earths, vol. 1-Metals, North-Holland Publishing Co., Amsterdam, 1978, p. 337.
[20] E. Gebhardt, I. Elssner, J. Hohler, J. Less-Common Met. 19 (1969) 329–335.
[21] O.D. Mcmasters, K.A. Gschneidner Jr., R.F. Venteicher, Acta Crystallogr. B 26 (1970) 1224–1229.
[22] J. Bijvoet, A.J. Van Dam, F. Van Beek, Solid State Commun. 4 (1966) 455–458.
[23] P.E. Blöchl, Phys. Rev. B 50 (1994) 17953–17979.
[24] G. Kresse, J. Joubert, Phys. Rev. B 59 (1999) 1758–1775.
[25] G. Kresse, J. Furthmuller, Phys. Rev. B 54 (1996) 11169–11186.
[26] G. Kresse, J. Furthmuller, Comput. Mater. Sci. 6 (1996) 15–50.
[27] J.P. Perdew, Y. Wang, Phys. Rev. B 45 (1992) 13244–13249.
[28] J.P. Perdew, J.A. Chevary, S.H. Vosko, K.A. Jackson, M.R. Pederson, D.J. Singh, et al., Phys. Rev. B 46 (1992) 6671–6687.
[29] Y. Wang, S. Curtarolo, C. Jiang, R. Arroyave, T. Wang, G. Ceder, L.Q. Chen, Z.K. Liu, CALPHAD 28 (2004) 79–90.
[30] M.E. Straumanis, S.M. Riad, Trans. Metall. Soc. AIME 233 (1965) 964–967.
[31] A.V. Morozkin, J. Alloys Compd. 345 (2002) 155–157.
[32] S. Steeb, D. Godel, C. Lohr, J. Less-Common Met. 15 (1968) 137–141.
[33] P. Morin, J. Pierre, Phys. Status Solidi A 21 (1974) 161–166.
[34] J. Pierre, R. Pauthenet, J. Appl. Phys. 34 (1963) 1971–1973.
[35] C.P. Wang, Z. Lin, X.J. Liu, J. Alloys Compd. 469 (2009) 123–128.
[36] Z.M. Du, D.H. Wang, W.J. Zhang, J. Alloys Compd. 284 (1999) 206–212.
[37] A.T. Dinsdale, CALPHAD 15 (1991) 317–425.
[38] A.K. Niessen, F.R. deBoer, R. Boom, P.F. deChatel, W.C.M. Mattens, A.R. Miedema, CALPHAD 7 (1983) 51–70.
[39] S. Delfino, A. Saccone, A. Borsese, R.Z. Ferro, Metallkd 17 (1976) 392–394.
[40] E. Gebhardt, M. Von Erdberg, J. Less-Common Met. 11 (1966) 141–147.
[41] M.I. Ivanov, G.M. Lukashenko, J. Less-Common Met. 133 (1987) 181–192.